Physical and Unphysical Causes of Nonstationarity in the Relationship between Barents-Kara Sea Ice and the North Atlantic Oscillation

Kristian Strommen[1] and Fenwick Cooper[1]

[1]Department of Physics, University of Oxford, UK

Key Points:

- A lack of observations means that ice-NAO links cannot be confidently assessed with reanalysis prior to the 1970s.
- Changes to the ice-NAO relationship are expected due to ice edge trends and the dependence of heatflux anomalies on ice edge variability.
- The location of the ice edge, and hence its potential influence on the NAO, varies across coupled climate models.

Corresponding author: Kristian Strommen, `kristian.strommen@physics.ox.ac.uk`

Abstract

The role of internal variability in generating an apparent link between autumn Barents-Kara sea ice (BKS) and the winter North Atlantic Oscillation (NAO) has been intensely debated. In particular, the robustness and causality of the link has been questioned by showing that BKS-NAO correlations exhibit nonstationarity in both reanalysis and climate model simulations. We show that the lack of ice observations makes analysis of nonstationarity using reanalysis questionable in the period 1950-1970 and effectively impossible prior to 1950. Model simulations are used to corroborate an argument that nonstationarity is nevertheless expected due to changes in the ice edge variability due to global warming. Consequently, changes in BKS-NAO correlations over time may simply reflect that the ice edge has moved, rather than that there is no causal link. We discuss potential implications for analysis based on coupled climate models, which exhibit large ice edge biases.

Plain Language Summary

Does the amount of ice in the Barents-Kara Sea influence European air pressure or are the patterns we see caused by random changes in the weather? In climate models and in estimates of the atmosphere's history these patterns change depending on which years we look at. This has been interpreted as evidence that the patterns are random. However, there are very few measurements of ice in this region before 1970, so we argue that looking at these years is not helpful. Since 1970, where we have more measurements, the winter sea ice edge has been moving Northwards because of global warming. When the ice in a particular region disappears, it changes the expected relationship with the atmosphere because heat can now quickly leave the ocean. Different climate models put the ice edge in different places and therefore cannot get this change correct.

1 Introduction

Many studies have suggested that anomalous Barents-Kara sea ice (BKS) in autumn can trigger predictable shifts in the winter North Atlantic Oscillation (NAO), and hence midlatitude winter weather (Deser et al., 2007; Sun et al., 2015; García-Serrano et al., 2015; Dunstone et al., 2016; Kretschmer et al., 2016; Wang et al., 2017; Caian et al., 2018). This teleconnection manifests as a positive correlation between autumn BKS and the winter NAO, with a reduction in sea ice appearing to force a negative NAO. However, there remains considerable scepticism in the literature on the robustness and even causality of this teleconnection.

One source of scepticism comes from modelling studies. Recent comprehensive studies using large ensembles show that coupled climate models largely reproduce such a positive BKS-NAO correlation over the satellite era (Blackport & Screen, 2021). However, the magnitude of the correlation is notably smaller in the models compared to estimates based on reanalysis (Blackport & Screen, 2021; Siew et al., 2021; Strommen et al., 2022), and there is considerable ensemble spread, with individual ensemble members simulating a wide range of positive and negative correlations (Koenigk & Brodeau, 2017; Blackport & Screen, 2021; Siew et al., 2021). Several studies have argued that this is because the BKS-NAO link seen in reanalysis data is largely reflecting atmospheric internal variability (Koenigk & Brodeau, 2017; Warner et al., 2020), and that the weak links simulated by coupled models may mostly reflect atmospheric forcing on the ice (Blackport & Screen, 2021).

Another source of scepticism arises from the work of Kolstad and Screen (2019) (hereafter KS19), who argue that there is clear evidence of nonstationarity (i.e., variation in time) in the BKS-NAO link in reanalysis data spanning the 20th century, with the recent period standing out as one of unusually high correlations. There is clearly much synergy between these two sources of scepticism, which could be jointly interpreted as suggesting that the apparently significant BKS-NAO correlation in the satellite era does not actually reflect a robust, causal relationship. Indeed, KS19 conclude by cautioning against using BKS as a statistical predictor of the NAO.

The purpose of this paper is to make two points concerning nonstationarity of BKS-NAO links, expanding on brief comments made in Strommen et al. (2022). Firstly, while it is well known that observations are sparser further back in time, the implications this may have for how confidently one can assess nonstationarity in reanalysis do not appear to have been commented on. Secondly, KS19 suggested that one cause of the apparent nonstationarity could be a dependence of the BKS-NAO link on the mean state, citing decadal North Atlantic variability as a potential source of such mean-state dependence. However, the potential role of global-warming induced changes to the sea ice was not mentioned. Here, we will argue:

1. That the lack of observations of autumn/winter sea ice means nonstationarity cannot be meaningfully assessed using reanalysis data extending further back than 1950, and is dubious even in the period 1950-1970.
2. That nonstationarity in BKS-NAO links is nevertheless expected because of changes to the ice edge over time (e.g. in response to global warming), but that such changes simply reflect that the sea ice region capable of exerting an influence on the NAO may have moved, rather than reflecting the lack of a robust and causal link between BKS and the NAO.

In the Discussion and Conclusions we will also comment on the potential implications of point 2 for analysis based on coupled models, known to exhibit considerable biases in their simulated ice edge.

2 Data and methods

2.1 Reanalysis and observational data

While KS19 considered three different reanalysis products to boost confidence in their analysis, here we only consider one of them, namely ERA20C (Poli et al., 2016). This is because all three reanalysis products considered in KS19 ultimately utilise the same sea ice data, namely HadISST (Titchner & Rayner, 2014); the sea ice in HadISST is itself primarily derived from the Walsh and Chapman dataset (Walsh & Chapman, 2001; Walsh et al., 2017). Since our focus is on the reliability of HadISST sea ice data, it thus suffices to use ERA20C. We also use ERA5 (Hersbach et al., 2020) when assessing CMIP6 model biases.

We assess the number of available observations in the Barents-Kara region over time prior to the satellite era (approximately 1979 onwards). To do so, we consider two sources of observations. Firstly, we use a count of the number of HadISST ship observations of sea surface temperatures (SST) over time. From this we computed the number of available observations in November anywhere within the Barents-Kara region (70-85N, 30-90E). This assumes that every ship visiting this region took a measurement of the sea ice, which is unlikely to be true. This is therefore best thought of as an upper bound on the true number. Secondly, we count the number of available ice edge charts from the Russian Arctic and Antarctic Research Institute (AARI) (Mahoney et al., 2008). We use the average number of charts available in the Barents-Kara region as our measure of chart availability. We note that the only other source of Barents-Kara observations used by Walsh and Chapman were charts collected by the Danish Meteorological Institute and the Arctic Climate System Study (Walsh et al., 2017). However, both these sources of charts only cover the summer months and so do not contribute to estimates of sea ice in October or November. The ship observations and AARI chart availability therefore provide a reasonable picture of the totality of available sea ice observations.

2.2 Model data

To assess how the ice-NAO link may depend on the ice edge mean state, we make use of an ensemble of coupled climate model simulations with stochastic ice and ocean parameterizations. This ensemble was introduced and studied in Strommen et al. (2022), and consists of 6 members spanning the period 1950-2015 using historical forcing data. The inclusion of stochastic parameterizations results in the model simulating consistently positive BKS-NAO correlations over the period 1980-2015 which are comparable in magnitude to that observed in reanalysis (Strommen et al., 2022). This close and consistent fidelity to observations is not observed in other model ensembles (Blackport & Screen, 2021; Siew et al., 2021), making it a valuable resource for studying the BKS-NAO link. Following Strommen et al. (2022), we will refer to this ensemble as OCE.

Details about the model configuration can be found in Strommen et al. (2022). In brief, the model used is based on the HighResMIP version of EC-Earth3 (Haarsma et al., 2020), itself based on a version of the Integrated Forecast System (IFS) developed and used at the European Centre for Medium Range Weather Forecasts (ECMWF). The ocean component uses NEMO version 3.6 (Madec & the NEMO team, 2016) which includes the LIM3 sea ice model (Vancoppenolle et al., 2012). Three stochastic ocean schemes (Juricke et al., 2017, 2018) and one stochastic sea ice scheme (Juricke et al., 2013; Juricke & Jung, 2014; Juricke et al., 2014) are included. The atmospheric model is run at a spectral resolution of T255, which roughly corresponds to 80km grid spacing at the equator, with 91 vertical layers. NEMO is run at a resolution of around 1° with 75 vertical layers.

2.3 Methods

We follow KS19 and define BKS as sea ice concentration averaged over the box 70-85N, 30-90E. We focus on November, rather than October as in KS19. The comparison with October will be discussed. The choice of November is motivated by the fact that correlations with both the NAO and European surface conditions peak in November and are more clearly significant then, unlike in October (García-Serrano et al., 2015; Santolaria-Otín et al., 2021). Furthermore, the physical pathway from October sea ice to the NAO appears to be primarily via its influence on November sea ice (García-Serrano et al., 2015; King et al., 2016; King & García-Serrano, 2016), with viable atmospheric pathways from November sea ice being more widely documented and studied (García-Serrano et al., 2015; Sun et al., 2015). Finally, seasonal forecasts of the winter NAO, such as those issued by ECMWF or the UK Met Office, are initialised using November initial conditions, making November BKS more relevant for actual forecasts. Thus, unless stated otherwise, informal references to ice, sea ice or BKS always refer to November sea ice concentration.

We define the NAO index in the OCE ensemble as the first principal component of 500hPa geopotential height; a daily principal component timeseries is detrended and has a seasonal cycle removed from it before DJF averages are taken. When correlating BKS with the NAO in the OCE ensemble, we concatenate all 6 members back to back before computing the correlation.

When determining statistical significance of correlations between sea ice and the NAO, our null-hypothesis models the DJF NAO as white noise and sea ice as an independent AR1 process with a lag of 1 years, in order to account for the high interannual autocorrelation in the ice. By fitting these models to the data and generating 1000 random timeseries, we can estimate p-values for the null hypothesis. Modelling the ice using a random Fourier phase shuffle method (Ebisuzaki, 1997), which preserves the autocorrelation at all lags, produced similar p-values.

All sea ice and heatflux (= sensible+latent) data are regridded onto a regular 1° grid before analysis is carried out. The heatflux sign convention is that "positive = upwards", i.e., heat flowing from the surface to the atmosphere.

3 Unphysical causes of nonstationarity: missing data

We begin by examining the impact of data availability. Figure 1(a) shows the November BKS timeseries in blue. It is immediately apparent that there is a dramatic difference in variability before and after 1950, with essentially zero variability before 1950. Figure 1(c) shows the November sea ice variance in the modern period 1980-2010 at all gridpoints in the Arctic, while 1(d) shows the same over the period 1900-1949. It is clear that the variability has vanished almost everywhere, not just in the Barents-Kara region. That this has a huge impact on assessments of ice-atmosphere interactions can be seen already at the level of the local interaction between two-metre temperature (T2M) and sea ice. The black line in Figure 1(a) shows correlations between BKS-averaged November T2M and November BKS for successive 30-year periods. A sharp discontinuity is apparent, with the correlations jumping from around -0.1 to -0.5 depending on whether the 30-year period includes years post-1950. The correlations drop again to ≈ -0.6 once the period includes years post-1980: note that this drop occurs even if trends in ice and T2M from 1990 onwards are removed, suggesting it is related to changes in variability and not global warming.

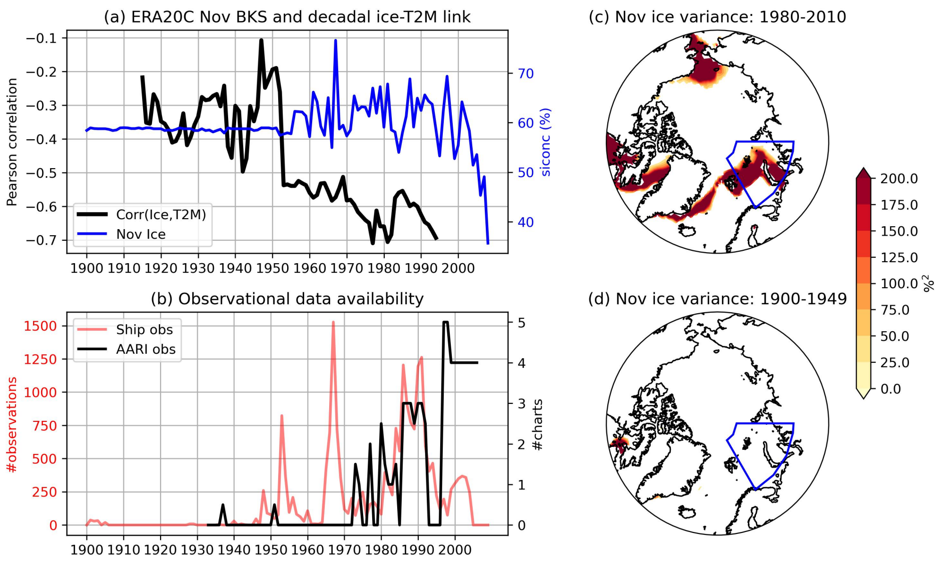

Figure 1. In (a): November BKS timeseries of ERA20C (blue) and successive 30-year correlations between November BKS and November T2M averaged over the same region (black). Each 30-year correlation is centred at the midpoint of the period (i.e. the point at 1965 corresponds to the period 1950-1980). In (b): total number of ship SST observations (red) and average number of AARI charts (black) over the Barents-Kara region. In (c): November interannual sea ice variance of ERA20C (1980-2010). In (d), the same but over the period 1900-1949. The blue boxes highlight the Barents-Kara region.

To understand these differences, Figure 1(b) shows the availability of observations from the Barents-Kara region over time. Prior to 1950 there are effectively zero observations in this region in November. Figure 1(d) suggests this lack of observations extends Arctic-wide and that the Walsh and Chapman data set consequently use a climatological value for the sea ice. Indeed, the documentation of the Walsh and Chapman data set explicitly states that it consists of "mostly climatologies before 1950". In the period 1950-1970, ship observations start becoming available, but there are no AARI charts. From around 1970 onwards AARI charts become more frequently available. From 1979 onwards satellite data becomes available.

We conclude that estimates of BKS-NAO correlations cannot be sensibly made prior to 1950 due to the total collapse of variability owing to missing observations, which leads to spurious unphysical effects in reanalysis already at the level of local ice-T2M links. While there are some ship observations available in the period 1950-1970, AARI observations are still lacking, and their availability from the 70s onwards also appears to project onto both the variability and estimates of ice-atmosphere links. The fact that sparse observations between 1950 and 1970 contaminates ice variability estimates is even more apparent in the monthly BKS timeseries, which exhibits visibly unphysical variability in this period (Figure S1 of the Supporting Information, SI). Estimates of BKS-NAO links prior to 1970 must therefore be interpreted with extreme caution.

KS19 focused on October BKS, while the above discussed November BKS. The collapse of past sea ice variability is somewhat less dramatic in October (see Figure S2), owing to slightly better availability of observations, but the difference is still considerable and again results in apparent nonstationarity in the ice-T2M link. KS19 do briefly comment on the reduced variability in the early 20th century: here we show that the extent and source of the reduction places serious limitations for how confidently nonstationarity can be assessed. Note that even if one takes the view that the October sea ice can be trusted prior to 1950, the total collapse of variability in November still severely limits the capacity of reanalysis to simulate a realistic BKS-NAO link, for the simple reason that any BKS anomaly present in October vanishes in November. Similarly, the sea ice evolution from October to November will be compromised by the lack of November observations in the period 1950-1970. If BKS anomalies really do force the NAO, biases in the October-November evolution would lead to biases in the NAO response. This point is further emphasised by the aforementioned studies suggesting that the reason October BKS anomalies appear to affect the NAO is because the October ice preconditions the November ice, with the actual forcing onto the NAO originating from the November ice anomaly (García-Serrano et al., 2015; King et al., 2016; King & García-Serrano, 2016). Thus, we argue that October BKS-NAO links also must be treated with extreme caution prior to 1970. We conclude that the nonstationarity reported by KS19 using reanalysis data does not constitute strong evidence against the existence of a robust and causal BKS-NAO teleconnection.

4 Physical causes of nonstationarity: a changing ice edge

The position of the Arctic ice edge has changed over time, primarily due to global warming, which has led to a gradual retreat of the edge (Stroeve & Notz, 2018; Notz & Community, 2020a). This is well reproduced by coupled climate models, including the OCE ensemble. Figure 2(a) shows the mean state of the OCE ensemble in the period 1950-1980, and Figure 2(b) the change between this period and the more recent period 1980-2015, demonstrating this retreat of the ice edge. Changes in the mean ice edge have immediate implications for changes to Arctic variability. This is because the interior of the Arctic is entirely frozen every November ($\approx 100\%$ sea ice concentration) and thus experiences zero interannual variability. Instead all interannual variability is concentrated at the ice edge. This is shown in Figures 2(c) and (d), showing November variance in the period 1950-1980 and the difference in the modern period. As the ice edge retreats, the regions experiencing considerable variability therefore also retreat.

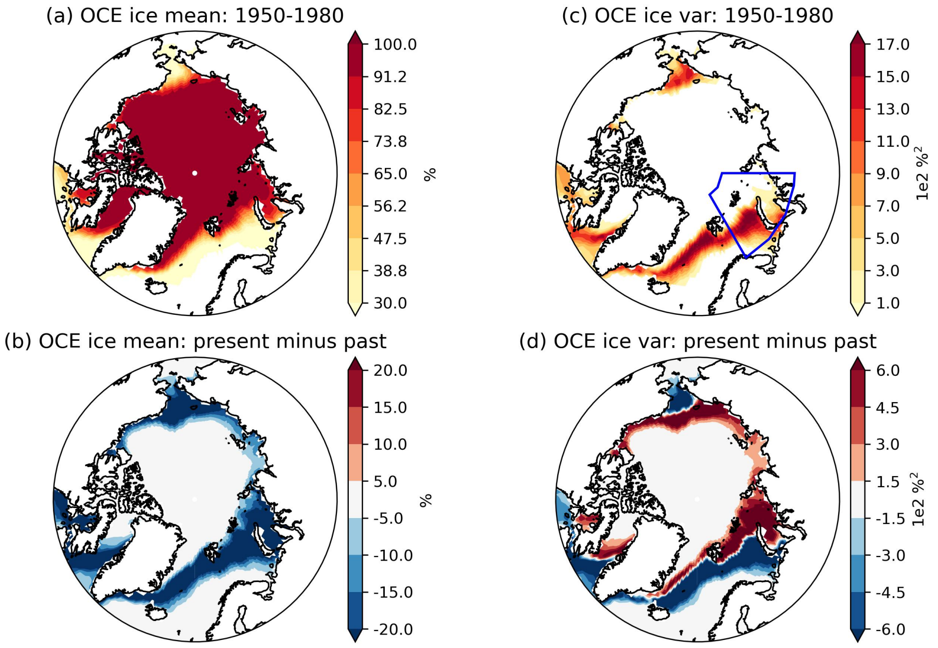

Figure 2. In (a): the mean November sea ice across the OCE ensemble in the period 1950-1980. In (b): the difference in the ice mean between 1980-2015 and 1950-1980. In (c) and (d): the same but for the variance rather than the mean. The blue box in (c) highlights the Barents-Kara region.

Physical reasoning implies that such changes to the ice edge variability will impact teleconnections from the Arctic to the NAO, because the teleconnection is mediated via heatfluxes. A negative sea ice anomaly may result in comparatively warm Arctic waters being exposed to cold air aloft, and the resulting thermal contrast can trigger heatflux anomalies as high as $500Wm^{-2}$ (Koenigk et al., 2009). These heatflux anomalies generate circulation anomalies that can propagate to the lower latitudes, via tropospheric (Deser et al., 2007) and/or stratospheric (Sun et al., 2015) pathways. Crucially, significant ice-induced heatflux anomalies can only occur at or near the ice edge, since (i) this is the only place where anomalous ice can expose or cover up the ocean, and (ii) this is the only place where ice variability occurs at all. This is demonstrated using the OCE ensemble in Figure 3(a), which shows the 1950-1980 interannual heatflux variability at gridpoints with a mean sea ice concentration of at least 5%. The heatflux variability is co-located with the 1950-1980 ice edge, and retreats in tandem with the edge under global warming (Figure 3(b)).

If Arctic sea ice really is capable of forcing the NAO, the above discussion suggests that the exact region of the Arctic responsible changes over time. In fact, this is what seems to happen in the OCE ensemble. Figure 3(c) and (d) show correlations between the winter NAO and November sea ice at every gridpoint for the two time periods. In the earlier period 1950-1980, significant correlations are found in the Barents sea, Greenland sea, and the coast of Greenland more broadly. These correlations are co-located with the peak heatflux variability associated with the more extended ice edge of that period. No correlations are found in the Kara sea, consistent with the fact that in OCE the Kara sea is almost permanently ice covered in November in the period 1950-1980, and thus

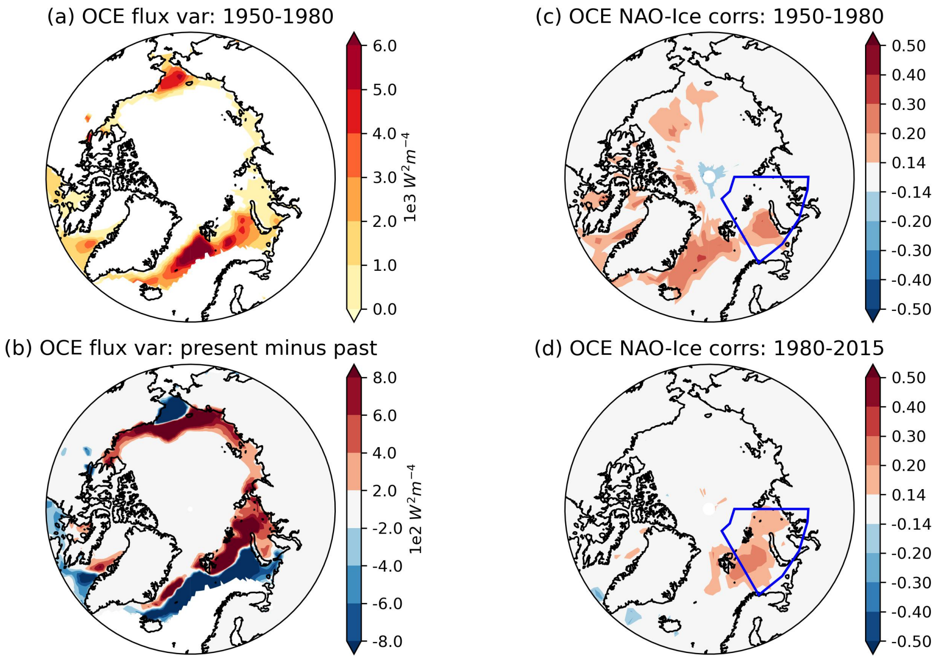

Figure 3. In (a): the average November heatflux variance across the OCE ensemble in the period 1950-1980. In (b): the difference in the heatflux variance between 1980-2015 and 1950-1980. In (c): correlations between the DJF NAO and November sea ice concentration at gridpoints in the period 1950-1980 using the OCE ensemble. In (d): the same but over the period 1980-2015. In (c) and (d) all gridpoints outside the zero contour are significantly different from our null-hypothesis ($p < 0.05$). The blue boxes highlight the Barents-Kara region. The heatflux sign convention is "positive = upwards".

experiences little/no ice or heatflux variability (Figure 2(a) and 3(a)). In the later period 1980-2015, correlations are still found in the Barents sea, but have largely vanished from around Greenland, consistent with the retreat of the ice and subsequent loss of heatflux variability there. On the other hand, the retreating ice edge in OCE means that the Kara sea has now become partially exposed, with roughly 23% of the model gridpoints in this region now experiencing ice concentrations of less than 5% every year. The OCE ensemble now also shows significant correlations in this region.

To summarise: (i) physical reasoning suggests that the regions capable of exerting a significant forcing on the atmosphere should be co-located with the ice edge, which is nonstationary due to global warming; (ii) the OCE ensemble precisely simulates such a nonstationary forcing. What does this imply for the BKS-NAO link? As noted, the November Kara sea ice is incapable of contributing notably to atmospheric forcing in the earlier period by virtue of being almost permanently ice covered, but as it slowly becomes more exposed begins contributing significant heatflux anomalies. The Barents sea contributes significantly and similarly during both periods. Thus one would naively expect that the total atmospheric forcing from the combined Barents and Kara seas would appear to increase over the period 1950 to present. In fact, this is precisely what happens in the OCE ensemble. The BKS-NAO correlation of the concatenated members ($N = 210$) is 0.13 ($p \approx 0.05$) in the earlier period, with individual members showing correlations above and below zero, and rises to 0.24 ($p \ll 0.05$) in the modern period, with all members exhibiting positive correlations.

We would like to stress that our remarks on the relationship between the ice edge and heatfluxes are in no way novel, and many studies have emphasised that the Barents and Kara sea appear to be important by virtue of being where the maximum ice edge variability takes place (Deser et al., 2000; Vinje, 2001; Koenigk et al., 2009). However, the implications this has for nonstationarity of teleconnections do not appear to have been made in the literature before.

5 Discussion

We highlight that the lack of observations implies nonstationarity in the BKS-NAO link cannot be confidently assessed using reanalysis. We therefore relied on climate model simulations to corroborate our proposed source of nonstationarity. It is nevertheless interesting to note that the nonstationarity KS19 report in the period 1950-2015 using reanalysis shows a BKS-NAO correlation slowly increasing from around 0 to around 0.4, and therefore appears consistent with the analysis of Section 4. Computation of gridpoint correlations between November sea ice and the NAO over the period 1950-1980 shows that ERA20C has significant correlations ($p < 0.05$) in the Greenland sea, but in contrast to OCE the sign of the correlation is negative (Figure S3). We note that there is no a priori reason why forcing from Greenland sea ice in the past should have a particular sign, with several studies emphasising that different regions of the Arctic may affect the NAO very differently (Rinke et al., 2013; Sun et al., 2015; Pedersen et al., 2016; Koenigk et al., 2016). To the extent that the ERA20C correlations can be taken seriously, their difference to OCE could be a result of a different climate mean state (Deser et al., 2007; Strong & Magnusdottir, 2010); for example, differences in the climatological position of the jet may easily result in forcing from the same geographical region affecting the jet differently (Baker et al., 2017, 2019). There are several outstanding questions about the pathways of Arctic teleconnections (Strommen et al., 2022) which would need to be answered to understand this better.

The fact that Arctic teleconnections may be linked to the location and variability of the ice edge is not just relevant for nonstationarity in time, but also has potential implications for model studies. It is well known that models exhibit considerable biases in both the mean and variability of Arctic sea ice (Koenigk et al., 2014; Roach et al., 2018; Notz & Community, 2020b; Gastineau et al., 2020; Watts et al., 2021; Khosravi et al., 2022). It follows that the precise Arctic regions capable of forcing the NAO may vary from model to model. Most studies using models apply a pre-defined BKS region to both reanalysis and models alike (Kolstad & Screen, 2019; Blackport & Screen, 2021; Siew et al., 2021). While this avoids potential "cherrypicking", it also risks exaggerating the weakness of model signals. For example, given a model with a strong forcing from the Barents sea but no forcing from the Kara sea (e.g. due to the model simulating a permanently ice-covered Kara sea), a correlation based on the Barents-Kara sea could give a misleading impression. Figure 4 demonstrates that CMIP6 models cannot be assumed to exhibit non-trivial sea ice variability in either the Barents or Kara seas. It seems of clear interest to assess how ice edge biases may affect model teleconnections, and furthermore to develop methods that allow for a more objective, physically motivated way to identify which Arctic regions may be forcing the NAO in a given model.

The behaviour of the OCE model corroborated our physical reasoning for nonstationarity, but this might be a particular feature of OCE which other models do not replicate. This could be because biases in sea ice variability or ice-atmosphere-ocean coupling mean that most coupled models are unable to simulate a teleconnection from any Arctic region whatsoever (Mori et al., 2019; Strommen et al., 2022). However, while the OCE ensemble appears to be uniquely good at replicating the observed BKS-NAO correlations, we emphasise that the reasons for this are still poorly understood, and caution must therefore be shown in interpreting the analysis presented here using the OCE ensemble

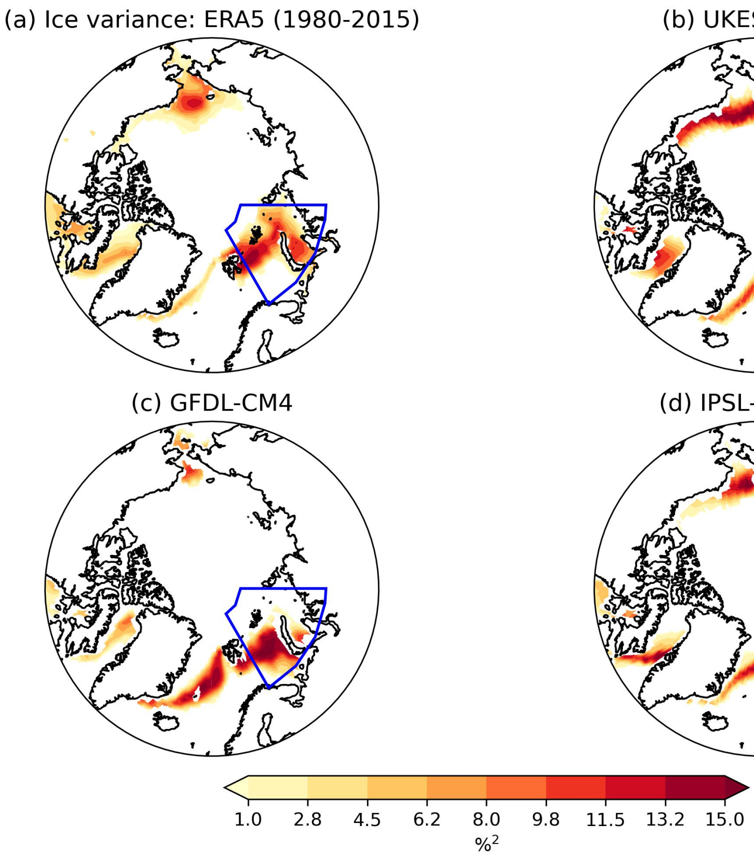

Figure 4. Interannual November sea ice concentration variance over the period 1980-2015 for (a) the ERA5 reanalysis, (b)-(d) three different coupled CMIP6 models (historical forcing scenario). The models have been hand-selected for being illustrative. The Barents-Kara region is highlighted with blue boxes.

6 Conclusions

KS19 argued that there is clear evidence of nonstationarity in the BKS-NAO link, and concluded that the link is non-robust and potentially non-causal. We have shown that the total lack of observations in the Barents and Kara seas prior to 1950 makes the assessment of nonstationarity prior to 1950 effectively impossible, and that the sparsity of November observations in the period 1950-1970 means correlations computed in this period must be treated with extreme caution. We therefore argue that the apparent non-stationarity reported by KS19 using reanalysis data cannot be used as evidence against the existence of a robust and causal BKS-NAO teleconnection.

Nevertheless, we have argued that simple physical reasoning suggests nonstationarity is to be expected due to changes in the ice edge over time due to global warming, since the location and variability of the ice edge determines the location of the heatflux anomalies responsible for generating Arctic signals. Importantly, while this does suggest that BKS-NAO correlations may have been lower in the past, it would be wrong to conclude from this that there is no robust and causal forcing on the NAO from BKS in recent decades. Rather, it may simply reflect that ice-edge changes means some regions, like the Greenland sea, are more important in the past, and some are less important, like the Kara sea. These arguments were corroborated using climate model simulations which exhibit strong correlations from the Barents-Kara region to the NAO in the period 1980-2015, which move along with the ice edge to the Greenland-Barents region in the period 1950-1980. In other words, Arctic sea ice may have been causally forcing the NAO across the entire 20th century, just not always from the same place.

We argue that model biases in the ice edge may have obfuscated a clear understanding of Arctic-NAO teleconnections in multi-model studies which prescribe the Barents-Kara region upfront, and this is a clear avenue of future research. Finally, our analysis has potential implications for future predictability of the NAO, since as the ice edge continues to retreat, the potential for large interannual sea ice variability decreases. This could mean decreased winter NAO predictability in a warming climate.

7 Open Research

The number of HadISST ship observations can be downloaded courtesy of the UK Met Office from `https://www.metoffice.gov.uk/hadobs/hadisst/data/download.html`. AARI chart availability is included in the NSIDC data set with DOI:10.7265/N5W37T8Z. It can be downloaded from `https://nsidc.org/data/g02182/versions/1`.

ERA20C data is available via the ECMWF Archive Catalogue: `https://apps.ecmwf.int/archive-catalogue/` The catalogue is public but to download the data you need to request access from ECMWF. ERA5 data is publicly available via the Copernicus Data Store.

Data for the first three ensemble members of OCE is publicly available on Zenodo, via the DOI https://doi.org/10.5281/zenodo.5256102.

CMIP6 data (Eyring et al., 2016) can be freely downloaded from the ESGF at `https://esgf-node.llnl.gov/projects/cmip6/`. We acknowledge the World Climate Research Programme, which, through its Working Group on Coupled Modelling, coordinated and promoted CMIP6. We thank the climate modeling groups for producing and making available their model output, the Earth System Grid Federation (ESGF) for archiving the data and providing access, and the multiple funding agencies who support CMIP6 and ESGF.

Acknowledgments

KS acknowledges funding from the Horizon Europe grant “EERIE” (grant agreement 101081383). FC acknowledges funding from the European Research Council under the EU’s Horizon 2020 programme (grant agreement 741112). We thank John Walsh for helpful comments on sea ice observations.

References

Baker, H. S., Woollings, T., Forest, C. E., & Allen, M. R. (2019). The linear sensitivity of the North Atlantic Oscillation and eddy-driven jet to SSTs. *Journal of Climate*, *32*(19), 6491–6511.

Baker, H. S., Woollings, T., & Mbengue, C. (2017). Eddy-driven jet sensitivity to diabatic heating in an idealized GCM. *Journal of Climate*, *30*(16), 6413–6431.

Blackport, R., & Screen, J. A. (2021). Observed Statistical Connections Overestimate the Causal Effects of Arctic Sea Ice Changes on Midlatitude Winter Climate. *Journal of Climate*, *34*(8), 3021 - 3038. doi: 10.1175/JCLI-D-20-0293.1

Caian, M., Koenigk, T., Döscher, R., & Devasthale, A. (2018). An interannual link between Arctic sea-ice cover and the North Atlantic Oscillation. *Climate Dynamics*, *50*(1), 423–441. doi: 10.1007/s00382-017-3618-9

Deser, C., Tomas, R. A., & Peng, S. (2007). The Transient Atmospheric Circulation

Response to North Atlantic SST and Sea Ice Anomalies. *Journal of Climate*, *20*(18), 4751 - 4767. doi: 10.1175/JCLI4278.1

Deser, C., Walsh, J. E., & Timlin, M. S. (2000). Arctic sea ice variability in the context of recent atmospheric circulation trends. *Journal of Climate*. doi: 10.1175/1520-0442(2000)013⟨0617:ASIVIT⟩2.0.CO;2

Dunstone, N., Smith, D., Scaife, A., Hermanson, L., Eade, R., Robinson, N., ... Knight, J. (2016). Skilful predictions of the winter North Atlantic Oscillation one year ahead. *Nature Geoscience*, *9*(11), 809–814. doi: 10.1038/ngeo2824

Ebisuzaki, W. (1997). A method to estimate the statistical significance of a correlation when the data are serially correlated. *Journal of climate*, *10*(9), 2147–2153.

Eyring, V., Bony, S., Meehl, G. A., Senior, C. A., Stevens, B., Stouffer, R. J., & Taylor, K. E. (2016). Overview of the Coupled Model Intercomparison Project Phase 6 (CMIP6) experimental design and organization. *Geoscientific Model Development*, *9*(5), 1937–1958.

García-Serrano, J., Frankignoul, C., Gastineau, G., & de la Cámara, A. (2015). On the Predictability of the Winter Euro-Atlantic Climate: Lagged Influence of Autumn Arctic Sea Ice. *Journal of Climate*, *28*(13), 5195 - 5216. doi: 10.1175/JCLI-D-14-00472.1

Gastineau, G., Lott, F., Mignot, J., & Hourdin, F. (2020). Alleviation of an Arctic sea ice bias in a coupled model through modifications in the subgrid-scale orographic parameterization. *Journal of Advances in Modeling Earth Systems*, *12*(9), e2020MS002111.

Haarsma, R., Acosta, M., Bakhshi, R., Bretonnière, P.-A., Caron, L.-P., Castrillo, M., ... Wyser, K. (2020). HighResMIP versions of EC-Earth: EC-Earth3P and EC-Earth3P-HR – description, model computational performance and basic validation. *Geoscientific Model Development*, *13*(8), 3507–3527. doi: 10.5194/gmd-13-3507-2020

Hersbach, H., Bell, B., Berrisford, P., Hirahara, S., Horányi, A., Muñoz-Sabater, J., ... Thépaut, J.-N. (2020). The ERA5 global reanalysis. *Quarterly Journal of the Royal Meteorological Society*, *146*(730), 1999-2049. Retrieved from `https://rmets.onlinelibrary.wiley.com/doi/abs/10.1002/qj.3803` doi: https://doi.org/10.1002/qj.3803

Juricke, S., Goessling, H. F., & Jung, T. (2014). Potential sea ice predictability and the role of stochastic sea ice strength perturbations. *Geophysical Research Letters*, *41*(23), 8396-8403. doi: https://doi.org/10.1002/2014GL062081

Juricke, S., & Jung, T. (2014). Influence of stochastic sea ice parametrization on climate and the role of atmosphere-sea ice-ocean interaction. *Philosophical Transactions of the Royal Society A: Mathematical, Physical and Engineering Sciences*, *372*(2018). doi: 10.1098/rsta.2013.0283

Juricke, S., Lemke, P., Timmermann, R., & Rackow, T. (2013). Effects of stochastic ice strength perturbation on arctic finite element sea ice modeling. *Journal of Climate*, *26*(11), 3785 - 3802. doi: 10.1175/JCLI-D-12-00388.1

Juricke, S., MacLeod, D., Weisheimer, A., Zanna, L., & Palmer, T. N. (2018). Seasonal to annual ocean forecasting skill and the role of model and observational uncertainty. *Quarterly Journal of the Royal Meteorological Society*, *144*(715), 1947-1964. doi: https://doi.org/10.1002/qj.3394

Juricke, S., Palmer, T. N., & Zanna, L. (2017). Stochastic Subgrid-Scale Ocean Mixing: Impacts on Low-Frequency Variability. *Journal of Climate*, *30*(13), 4997 - 5019. doi: 10.1175/JCLI-D-16-0539.1

Khosravi, N., Wang, Q., Koldunov, N., Hinrichs, C., Semmler, T., Danilov, S., & Jung, T. (2022). The Arctic Ocean in CMIP6 models: Biases and projected changes in temperature and salinity. *Earth's Future*, *10*(2), e2021EF002282.

King, M. P., & García-Serrano, J. (2016). Potential ocean–atmosphere preconditioning of late autumn Barents-Kara sea ice concentration anomaly. *Tellus A: Dy-*

namic Meteorology and Oceanography, *68*(1), 28580.

King, M. P., Hell, M., & Keenlyside, N. (2016). Investigation of the atmospheric mechanisms related to the autumn sea ice and winter circulation link in the Northern Hemisphere. *Climate dynamics*, *46*, 1185–1195.

Koenigk, T., & Brodeau, L. (2017). Arctic climate and its interaction with lower latitudes under different levels of anthropogenic warming in a global coupled climate model. *Climate Dynamics*, *49*(1), 471–492.

Koenigk, T., Caian, M., Nikulin, G., & Schimanke, S. (2016). Regional Arctic sea ice variations as predictor for winter climate conditions. *Climate Dynamics*, *46*(1), 317–337. doi: 10.1007/s00382-015-2586-1

Koenigk, T., Devasthale, A., & Karlsson, K.-G. (2014). Summer Arctic sea ice albedo in CMIP5 models. *Atmospheric Chemistry and Physics*, *14*(4), 1987–1998.

Koenigk, T., Mikolajewicz, U., Jungclaus, J. H., & Kroll, A. (2009). Sea ice in the Barents Sea: seasonal to interannual variability and climate feedbacks in a global coupled model. *Climate Dynamics*, *32*(7), 1119–1138.

Kolstad, E. W., & Screen, J. A. (2019). Nonstationary Relationship Between Autumn Arctic Sea Ice and the Winter North Atlantic Oscillation. *Geophysical Research Letters*, *46*(13), 7583-7591. doi: https://doi.org/10.1029/2019GL083059

Kretschmer, M., Coumou, D., Donges, J. F., & Runge, J. (2016). Using Causal Effect Networks to Analyze Different Arctic Drivers of Midlatitude Winter Circulation. *Journal of Climate*, *29*(11), 4069 - 4081. doi: 10.1175/JCLI-D-15-0654.1

Madec, G., & the NEMO team. (2016). NEMO ocean engine version 3.6 stable. *Note du Pôle de modélisation de l'Institut Pierre-Simon Laplace*, *27*.

Mahoney, A. R., Barry, R. G., Smolyanitsky, V., & Fetterer, F. (2008). Observed sea ice extent in the Russian Arctic, 1933–2006. *Journal of Geophysical Research: Oceans*, *113*(C11).

Mori, M., Kosaka, Y., Watanabe, M., Taguchi, B., Nakamura, H., & Kimoto, M. (2019). Reply to: Is sea-ice-driven Eurasian cooling too weak in models? *Nature Climate Change*, *9*(12), 937–939. doi: 10.1038/s41558-019-0636-0

Notz, D., & Community, S. (2020a). Arctic Sea Ice in CMIP6. *Geophysical Research Letters*, *47*(10), e2019GL086749. (e2019GL086749 10.1029/2019GL086749) doi: https://doi.org/10.1029/2019GL086749

Notz, D., & Community, S. (2020b). Arctic sea ice in CMIP6. *Geophysical Research Letters*, *47*(10), e2019GL086749.

Pedersen, R. A., Cvijanovic, I., Langen, P. L., & Vinther, B. M. (2016). The impact of regional Arctic sea ice loss on atmospheric circulation and the NAO. *Journal of Climate*, *29*(2), 889–902.

Poli, P., Hersbach, H., Dee, D. P., Berrisford, P., Simmons, A. J., Vitart, F., ... others (2016). ERA-20C: An atmospheric reanalysis of the twentieth century. *Journal of Climate*, *29*(11), 4083–4097.

Rinke, A., Dethloff, K., Dorn, W., Handorf, D., & Moore, J. (2013). Simulated Arctic atmospheric feedbacks associated with late summer sea ice anomalies. *Journal of Geophysical Research: Atmospheres*, *118*(14), 7698–7714.

Roach, L. A., Dean, S. M., & Renwick, J. A. (2018). Consistent biases in Antarctic sea ice concentration simulated by climate models. *The Cryosphere*, *12*(1), 365–383.

Santolaria-Otín, M., García-Serrano, J., Ménégoz, M., & Bech, J. (2021). On the observed connection between Arctic sea ice and Eurasian snow in relation to the winter North Atlantic Oscillation. *Environmental Research Letters*, *15*(12), 124010.

Siew, P. Y. F., Li, C., Ting, M., Sobolowski, S. P., Wu, Y., & Chen, X. (2021). North Atlantic Oscillation in winter is largely insensitive to autumn

Barents-Kara sea ice variability. *Science Advances*, *7*(31), eabg4893. doi: 10.1126/sciadv.abg4893

Stroeve, J., & Notz, D. (2018). Changing state of Arctic sea ice across all seasons. *Environmental Research Letters*, *13*(10), 103001. doi: 10.1088/1748-9326/aade56

Strommen, K., Juricke, S., & Cooper, F. (2022). Improved teleconnection between Arctic sea ice and the North Atlantic Oscillation through stochastic process representation. *Weather and Climate Dynamics*, *3*(3), 951–975.

Strong, C., & Magnusdottir, G. (2010). The Role of Rossby Wave Breaking in Shaping the Equilibrium Atmospheric Circulation Response to North Atlantic Boundary Forcing. *Journal of Climate*, *23*(6), 1269 - 1276. doi: 10.1175/2009JCLI2676.1

Sun, L., Deser, C., & Tomas, R. A. (2015). Mechanisms of Stratospheric and Tropospheric Circulation Response to Projected Arctic Sea Ice Loss. *Journal of Climate*, *28*(19), 7824 - 7845. doi: 10.1175/JCLI-D-15-0169.1

Titchner, H. A., & Rayner, N. A. (2014). The Met Office Hadley Centre sea ice and sea surface temperature data set, version 2: 1. Sea ice concentrations. *Journal of Geophysical Research: Atmospheres*, *119*(6), 2864–2889.

Vancoppenolle, M., Bouillon, S., Fichefet, T., Goosse, H., Lecomte, O., Morales Maqueda, M. A., & Madec, G. (2012). The Louvain-la-Neuve sea ice model. *Note du Pôle de modélisation de l'Institut Pierre-Simon Laplace*, *31*.

Vinje, T. (2001). Anomalies and Trends of Sea-Ice Extent and Atmospheric Circulation in the Nordic Seas during the Period 1864–1998. *Journal of Climate*, *14*(3), 255 - 267. doi: 10.1175/1520-0442(2001)014⟨0255:AATOSI⟩2.0.CO;2

Walsh, J. E., & Chapman, W. L. (2001). 20th-century sea-ice variations from observational data. *Annals of Glaciology*, *33*, 444–448.

Walsh, J. E., Fetterer, F., Scott Stewart, J., & Chapman, W. L. (2017). A database for depicting Arctic sea ice variations back to 1850. *Geographical Review*, *107*(1), 89–107.

Wang, L., Ting, M., & Kushner, P. J. (2017). A robust empirical seasonal prediction of winter NAO and surface climate. *Scientific Reports*, *7*(1), 279. doi: 10.1038/s41598-017-00353-y

Warner, J. L., Screen, J. A., & Scaife, A. A. (2020). Links Between Barents-Kara Sea Ice and the Extratropical Atmospheric Circulation Explained by Internal Variability and Tropical Forcing. *Geophysical Research Letters*, *47*(1), e2019GL085679. (e2019GL085679 2019GL085679) doi: https://doi.org/10.1029/2019GL085679

Watts, M., Maslowski, W., Lee, Y. J., Kinney, J. C., & Osinski, R. (2021). A spatial evaluation of Arctic sea ice and regional limitations in CMIP6 historical simulations. *Journal of Climate*, *34*(15), 6399–6420.